The 2013 World Congress on
Advances in Structural Engineering and Mechanics (ASEM13)
Jeju, Korea, September 8-12, 2013

Effect of the heat input in the mechanical and metallurgical properties of welds on AHSS transformed induced plasticity steel joined with GMAW process

*Victor-Lopez[1)], Arturo-Reyes[2)] and Patricia-Zambrano[3)]

[1), 2)] *Corporación Mexicana de Investigación en Materiales,Saltillo,Mexico*
[3)] *Universidad Autónoma de Nuevo Leon,Monterrey,Mexico*

[1)] *vlopez@comimsa.com*

ABSTRACT

The effect of the heat input on the mechanical and metallurgical properties of the welds has been investigated in the Heat Affected Zone (HAZ) of welds joints welded with GMAW, using the typical welding parameters for the normal production. The thermal effect in the HAZ of the welds is important for the optimization of the welding parameters used when weld TRIP steels are joined, because this will have a great influence in the final mechanical and metallurgical properties of the joint. In this work 3 samples was welded a High, Average and low heat input, with the variation of welding parameters to obtain different thermal affectation to investigate the variations in the parts of the joints: Weld, HAZ and Base Metal, due the heat applied for the welding process. Mechanical properties were evaluated by tension test, microhardness and fatigue testing and metallurgical evaluation with optical metallograpy, Scanning electron microscopy (SEM), fractograpy and X-ray Diffraction (XRD) to evaluate the transformation of retained austenite in the welds. The results obtained shows that the mechanical properties of the tension test decrease with the heat input increase and the microhardness exhibit a softening zone in the HAZ with lower hardness and the fatigue lives were also very similar for all heat inputs in the high stress levels only in low stress there is a differences. For metallurgical properties the metallographic evaluation shows ferrite, bainite , martensite and retained austenite, and the fractography analysis exhibit a ductile fracture in all cases and the content in volume fraction of retained austenite increases in the HAZ of welds with increasing heat input in to the base metal due the thermal effect.

1. INTRODUCTION.

Due to high demand in energy savings, safety and reduction of pollutant emissions in cars, Advanced High Strength Steels (AHSS) have become very attractive materials for use in the automotive industry. The weldability of Transformation Induced Plasticity steels (TRIP) is a technical challenge for its use in the manufacture of automotive components, especially when the performance of these structures welded must meet

[1)] MC
[2,3)] Ph.D

high quality and safety requirements.(Kapustka 2008)

The Gas Metal Arc Welding Process (GMAW) is the most commonly used in the automotive industry for joining conventional steels, however advanced TRIP steel does not offer this same facility to be welded; control of the welding parameters is critical in order to avoid the thermal effect of the welding process used, because cause microstructural changes in the original phases in detriment of desired mechanical properties in the weld joint.(Mei Zhang 2008).The welding parameters represent the acceptable range for proper control of Heat Input (HI) in the welded joint. The effect of this HI in the mechanical and metallurgical properties of the welds in TRIP steels in the HAZ of welds is studied in this paper.

TRIP steels differ of conventional steels in their chemical and mechanical properties, resulting multiphase microstructures such as ferrite, bainite and retained austenite traces, this structure transforms to martensite, improving higher mechanical properties, with less thickness equivalent in resistance of conventional steels (LI Zhuang 2007). Used for automotive safety components which absorb impact energy, transforming to martensite during crash.

In this study parameters were developed for high, average and low Heat Iinput values based on the average parameters used in normal production. Specimens were welded with this values to investigate the effect of the heat input on the mechanical and metallurgical properties of the welds due to the heat applied by the welding process in the HAZ of welded joints and these were evaluated by tension test, microhardness and fatigue testing and metallurgical evaluation with optical metallograpy, Scanning electron microscopy (SEM), fractograpy and X-ray Diffraction (XRD).

2. EXPERIMENTAL PROCEDURE.

For this study the Advanced High Strength Steel used was a Transformed Induced Plasticity (TRIP) steel grade 780 of 2.8 mm thickness that is currently used in auto body structures. A chemical analysis is 0.10 % C,1.98 % Mn, 2.35 % Si, 0.002 % S, 0.002 % P, 0.06 % Cr, 0.04% Ni,0.03 % Mo, 0.012 % Cu, 0.019 % V, 0.004 % Nb y 0.01 % Ti. and Mechanical properties of 854 MPa TS, 652 MPa YS and 20 % elongation.

For the realization of the welding coupons those was welded by the process of welding automatic GMAW we use a MOTOMAN robot model UP-20 and a power machine CLOOS GLC 553, shielding gas used was 90% Argon and 10% Co_2 a commonly used gas mixture in the automotive industry. Varying the welding parameters for test coupons we obtain Low, Average and High heat input, these welding parameters used was normally used in production lines, are shown in Table 1. Filler metal used was Lincoln ER70S-3 0.9 mm in diameter with a chemical composition of 0.08% C, 1.20% Mn, 0.55 Si, 0.008% P % and % 0.008 S and mechanical properties of 405 MPa Yield strength, 510 MPa Tensile strength and 26% elongation.

For the weld join design Lap joint was used in this work, because its wide used in joining auto-body structural components. A schematic of the weld joint design is shown in Fig. 1. The overlap between the two plates is 25.4mm. Clamps were used during welding to minimize the gap between the two overlapping plates. The tension test and fatigue test specimens were water jet cut from the welded plates. The dimensions of the specimen are shown in Fig. 2. In order to minimize specimen-to-specimen

Table 1 Welding Parameters

ID	Sample	Process	Filler Metal		Current			Welding Speed cm/min	Gas	Gas Flow (cfh)	Heat Input kJ/mm
			AWS	Ø (mm)	Polarity	Amp (A)	Volts (V)				
High	T36	GMAW	ER70S-3	0.09	CDEP	235-255	23.6	91.44	80% Ar-20%CO2	55	0.304
Average	T40	GMAW	ER70S-3	0.09	CDEP	235-255	23.6	101.6	80% Ar-20%CO2	55	0.273
Low	T44	GMAW	ER70S-3	0.09	CDEP	235-255	23.6	111.76	80% Ar-20%CO2	55	0.248

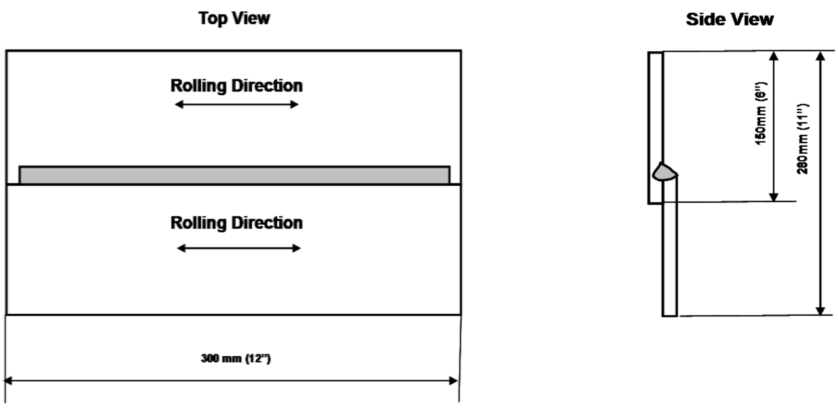

Fig. 1 Weld Plate Dimension

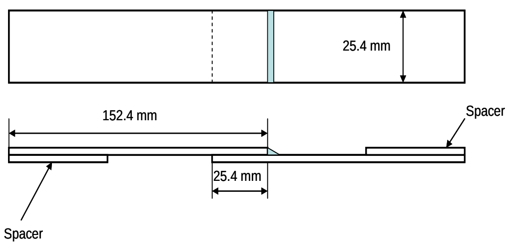

Fig. 2 Tension and Fatigue Test Specimen

variations in weld geometry profile and microstructure, all fatigue specimens for a given heat input analyzed were cut from one 300 mm long welded coupon, and the materials near the starts and stops were discarded.

An MTS 810 materials testing machine with 100 kN capacity was used for tensile and fatigue testing. Three tensile tests were performed for each heat input condition and peak loads were recorded. A pulling speed of 10 mm/s was used. Peak load data was used for fatigue test load selection. Fatigue testing was conducted using a constant amplitude sinusoidal load history with various load levels (R=0.1). Testing was suspended for specimens that survived 5 million cycles without fracture. All tests were conducted under ambient temperature. The complete separation of the specimen into two parts defines the cycles to failure. Cycles to failure and primary fatigue crack locations were recorded. Fig. 3 shows the setup for tensile and fatigue testing.

Fig. 3. Test Setup for Tensile and Fatigue Testing

One specimen from each heat input condition was cross sectioned, for metallographic evaluation samples, were prepared by abrasive cutting disc, grinding, polishing and etched with 5% Nital and evaluated with optical microscope for metallographic evaluation,

Macrophotos were taken to evaluate weld profiles and heat affected zone. Microhardness mapping tests were conducted for the high, average and low heat input conditions to evaluate the hardness changes in weld metal and heat affected zones. Traverse measurement was made across the weld and heat affected zone (HAZ) regions. Vickers hardness tests were conducted using a load level of 500g.

For microhardness testing a equipment Future Tech FM model was used doing a profile of Vickers microhardness with load of 500 g on Base Metal (BM), heat-affected zone (HAZ) and weld (SOL) to a depth of 1 mm from the surface of both the lower and upper plate, taking readings every 0.25 mm this in order to determine the effect of different thermal heat input measured hardness profile in the different zones evaluated for each specimen. Fig. 4 shows the position for making the hardness.

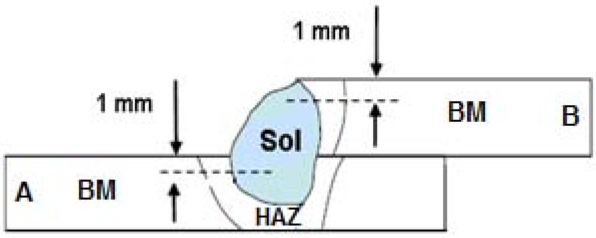

Fig. 4 Microhardness positions

In order to evaluate the thermal effect of the different Heat Input used in the welding coupons in the transformation of retained austenite in the HAZ of welded joints is conducting metallographic analysis and quantitative evaluation of retained austenite by X-Ray diffraction (XRD).

Retained austenite was determined on Base metal outside of the weld and HAZ with high and low Heat Input. Each sample consists of a fillet weld on lap joint mounted in Bakelite with polished metallographic preparation and etched with Nital. Each sample was mounted on a sample holder on a PANalytical X PERT diffractometer using Cu radiation at 45 kV and 40 mA. A scan was run in an angular range of 40 ° to 90 ° at intervals of 0.0157 ° and a count of 1.000 seconds per interval. The sample was aligned with the incidence of X-Ray beam and was perpendicular to the thin dimension of the weld overlap and outside centered at half of the HAZ, which was determined by a gage indicator. The incident angle used had a size of approximately 2 mm. Fig. 5.

Fig. 5 X-Ray equipment position of the sample

Once these collected data were analyzed in accordance with ASTM E975 and the reference data using the SAE SP-453 method. This method is known as direct comparison method uses intensity ranges austenite phase (γ phase) and ferrite phase (α phase) and the correction factors of the scattering intensity of each phase. The formula Eq (1) used to calculate the volume fraction (fγ) of the austenite phase is:

$$f^{\gamma} = \frac{I_1 R_2 / I_2 R_1}{(1 + I_1 R_2 / I_2 R_1)} \tag{1}$$

where:

f^{γ} = Volume fraction of austenite

I_1, I_2 = hkl peak intensity of austenite and ferrite, respectively

R_1, R_2 = Correction Factor for austenite and ferrite, respectively

The values are measured directly from the diffraction analysis, while the values of Ri are obtained in several published tables, the relevant part of tables is reproduced for Cu radiation below.

Ferrite (α)		**Austenite (γ)**	
hkl	**R_{α}**	**hkl**	**R_{γ}**
110	250	111	184
200	36	200	83
211	71	220	47
220	25	311	58

3. RESULTS AND DISCUSSION.

3.1 Tensile Test

The results obtained in the tension test for the maximum load obtained are shown in Fig. 6, where it can be seen that the increased strength of the weld is observed in the low values of heat input (T44) having a decreasing trend as thermal effect is increased due to increased heat input (T36) for reducing the speed of the robot during the application of welding, which we promotes greater thermal effect or softening zone in the heat affected zone with softer phases precipitation and grain microstructures with lower hardness, which is reflected in the values of tensile strength of the samples analyzed.

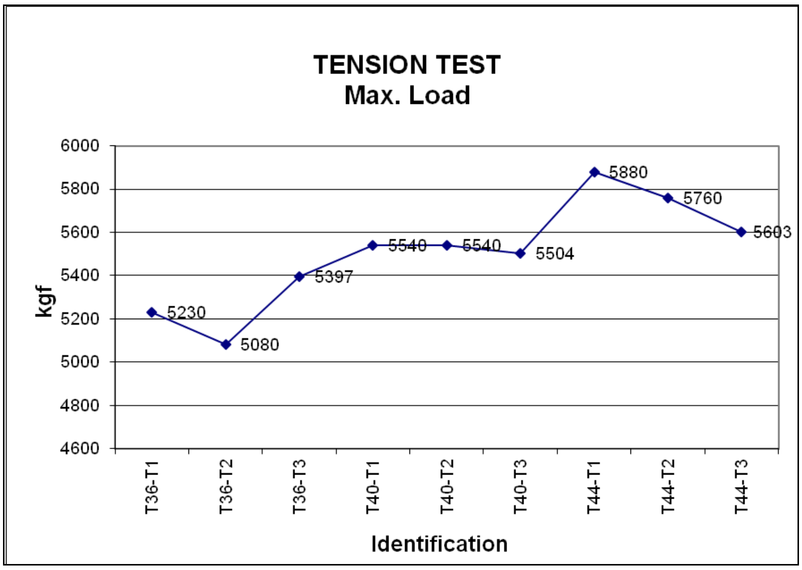

Fig. 6 Tension Test Max. Load

These results obtained for maximum load on tensile testing of welds, are converted to shear strength under AWS B4.0 guidelines with the following formula Eq (2) :

$$\tau = \frac{P}{l\ a} \tag{2}$$

Where:

$\mathbf{P}$ = Load

l = Total length of filler weld sheared

a = Theoretical throat dimension

τ = Shear strength of weld

The results are plotted and shown in Fig. 7 which shows a behavior similar to that seen in the chart above except that the behavior of shear stress.

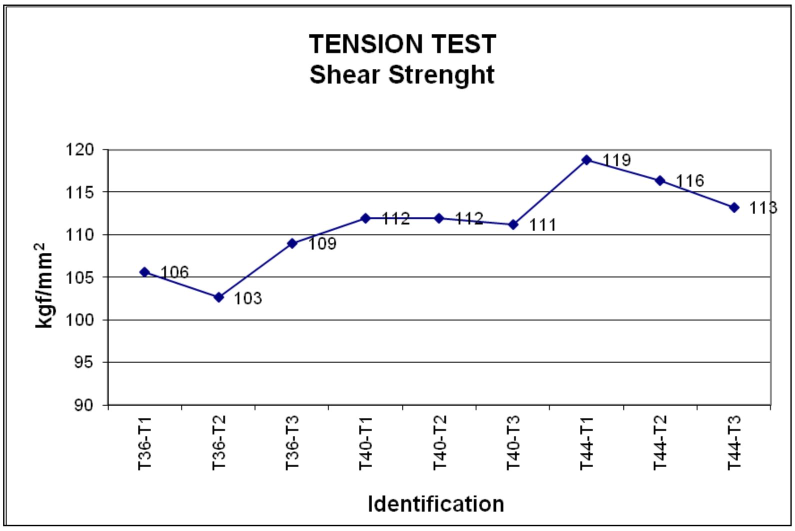

Fig. 7 Tension Test Shear Strenght

3.2 Microhardness

In Fig. 8 shows the hardness profiles obtained in the microhardness testing on Base Metal (BM), heat affected zone (HAZ) and weld (SOL) in the bottom plate (A) and the top plate (B). Yielding hardness values differ depending on the area in which they reside.

In the Base metal BM in all cases the hardness shows a downward trend until its lowest value in the transition zone with the start of the Heat Affected Zone HAZ (Softening Zone), obtaining minimum values of 232 and 228 HV for the specimen T36 BM-A and BM-B, 235 and 255 HV for the specimen T40 BM-A and BM-B, 260 and 263 HV for the specimen HV T44 BM-A and BM-B, which is an indication that the specimen with greater heat input T36 has greater sensitivity due to the thermal effect that the greater heat input to a slower cooling, which promotes the precipitation of higher percentage of the soft ferrite microstructures and decreased the original hardest structures as bainite in the base metal, which gives us an area of softening adjacent to the Heat Affected Zone HAZ. Noting that in this region the weld is decreasing its mechanical strength compared with hardness values of HV 312 originally obtained on average in Base Metal MB before being welded.

In the Heat Affected Zone (HAZ) is an increase of hardness in the transition from Base Metal (BM) with the Heat Affected Zone (HAZ) to the beginning of the melting zone of the Metal Base (BM) with the weld. Obtaining maximum values of 381 and 350 HV for Specimen T36 HAZ-A and HAZ B, 415 and 372 HV for Specimen T40 HAZ-A and HAZ -B, 446 and 417 HV for Specimen T44 HAZ -A and HAZ -B, which shows that the specimen with a heat input smaller T44, has higher hardness values, this due

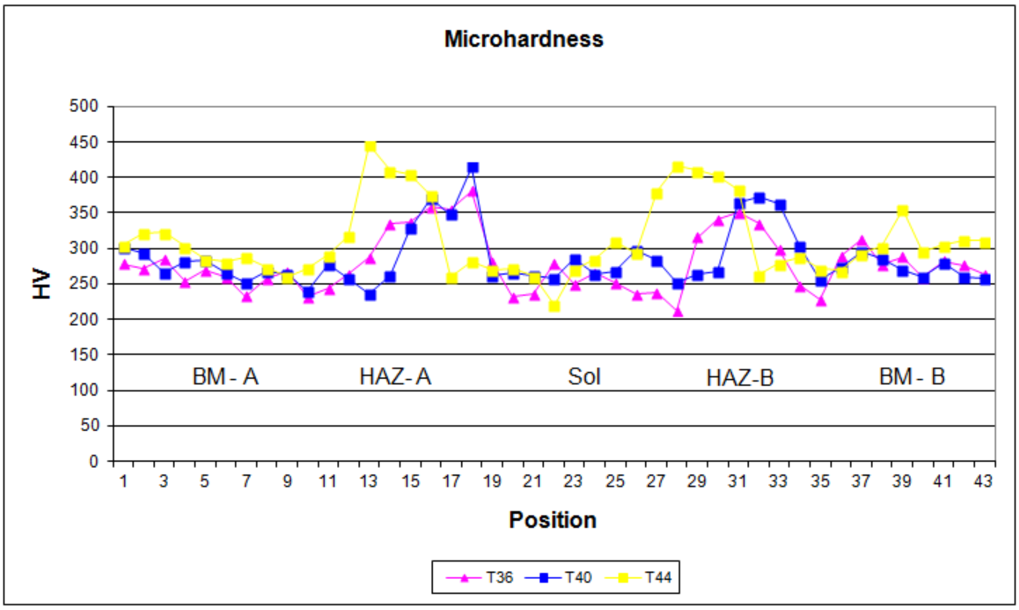

Fig. 8 Comparative hardness profile

to its increased sensitivity to thermal effect of the welding process due to its low heat input with higher cooling rates, which produces higher percentage and refinement of hard microstructures as bainite and martensite, which increases its mechanical strength in this area of the welded joint even higher than the base metal.

In the weld zone (Sol) obtained average hardness of 220 HV to T36, 247 HV to T40 and 248 HV to T44 specimens that are normal hardness of the filler metal used ER70S-6.

To analyze the behavior of the hardness in the most sensitive area to stress during fatigue testing, was performed microhardness mapping at the toe of the weld in the sample T36 High heat input and T44 Low heat input. Mapping results shown in Fig. 9 and 10 respectively.

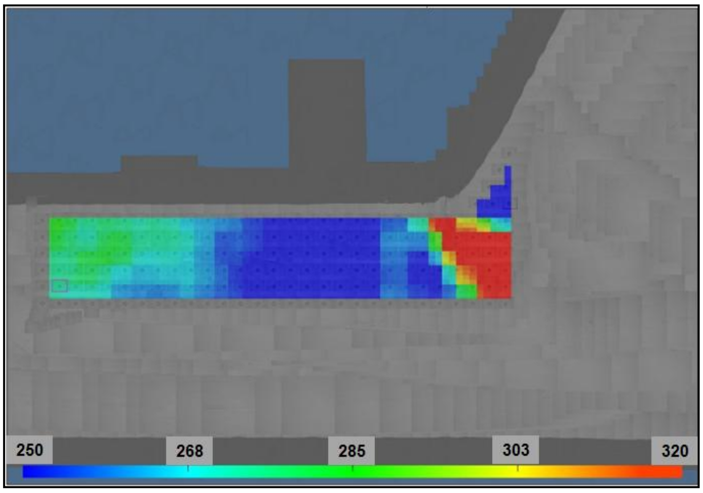

Fig. 9 Microhardness mapping T36 High heat input

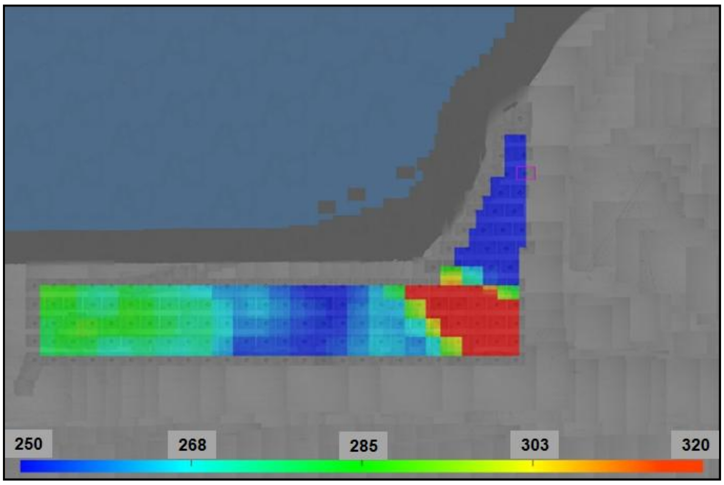

Fig. 10 Microhardness mapping T44 Low heat input

Table 2 Fatigue Test Data Low, Average And High Heat Input

ID	FATIGUE LOAD (N)	STRESS (Mpa)	CYCLES			FRACTURE LOCATION		
			Sample 1	Sample 2	Sample 3	Sample 1	Sample 2	Sample 3
T36	3,430	48.42	1,964,752	5000000 +	1,589,639	Toe	not broken	Toe
	4,000	56.47	1,212,192	1,159,992	680,318	Toe	Toe	Toe
	5,275	74.46	225,879	271,961	146,976	Toe	Toe	Toe
	10,550	148.93	23,447	34,272	21,409	Toe	Toe	Toe
	26,375	372.32	1,729	1,880	1,195	Toe	Toe/Root	Toe/Root
T40	3,430	48.42	1,956,104	1,654,279	1,541,279	Toe	Toe	Toe
	4,000	56.47	517,568	603,450	693,196	Toe	Toe	Toe
	5,275	74.46	236,564	198,720	173,616	Toe	Toe	Toe
	10,550	148.93	32,673	26,713	24,313	Toe	Toe	Toe
	26,375	372.32	1,574	1,681	1,305	Toe/Root	Toe/Root	Toe/Root
T44	3,430	48.42	967,450	1,680,066	1,761,724	Toe	Toe	Toe
	4,000	56.47	626,448	667,512	624,725	Toe	Toe	Toe
	5,275	74.46	154,476	216,875	173,616	Toe	Toe	Toe
	10,550	148.93	23,992	27,997	25,453	Toe	Toe	Toe
	26,375	372.32	1,666	1,543	1,734	Toe/Root	Toe/Root	Toe/Root

With the measurements obtained, was conducted to determine the matrix microhardness around the site of initiation of fatigue cracks in the weld toe. Test results show that the heat input welding under wider area T44 is hard due to higher cooling rates, which welds higher heat input T36 with slower cooling rates, that is a condition that depends on the velocity of movement during the application of welding. The effects of heat input in the softening of the heat affected zone is higher in specimen T36 high heat input with higher affected area.

3.3 Fatigue Test

The results obtained during the fatigue test are shown in Table 2, where we can observe the nominal loads and stresses applied to the weld tested specimens and the individual values of cycles to fracture and separation of the specimen.

S-N curves for the low, average, and high heat input conditions was build with the data of the table 1 by regression analysis and are shown in Fig. 11. Curves for Fatigue lives were also very similar for all heat inputs, with no significant differences observed. That means the use of high or low heat inputs doesn't have significant effect on fatigue life at high stress but at low stress there is a difference between the higher and lower cycles obtained at different heat input used in welding joints, due the welding speeds used in this study.

An analysis of fatigue life data from S-N curves can be determined that this means that the use of high or low heat inputs does not have a significant effect on the fatigue life of welded joints at high loads and stresses resulting low cycles fatigue life with minimal variation, but at low loads and stresses are obtained high cycles fatigue life, where there is a variation between cycles obtained in the heat inputs T44 and T36, having a greater fatigue life welding specimens with greater thermal effect by the high heat input T36, due to the presence of wide areas with microstructures with lower hardness, that the specimen T44 with lower thermal effect showing areas with higher hardness.

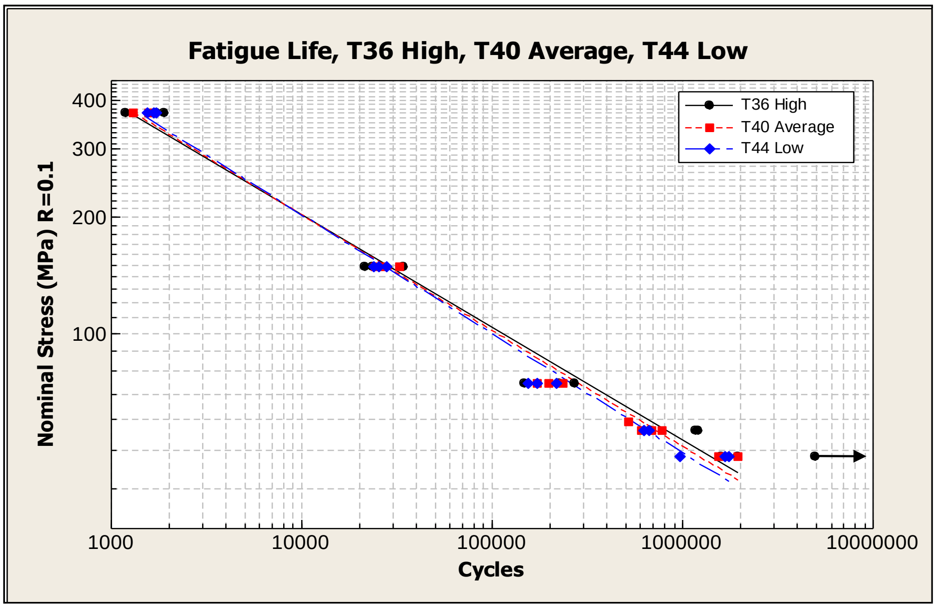

Fig. 11 S-N Curves Nominal Stress vs Cycles T36,T40 y T44

Fractures are present in two locations, including the weld toe and weld root. Just a high fatigue stress or low cycles the fractures are in the weld root, for the high stress concentration due the sample weld geometry. Photos of fractured fatigue specimens are shown in Fig. 12.

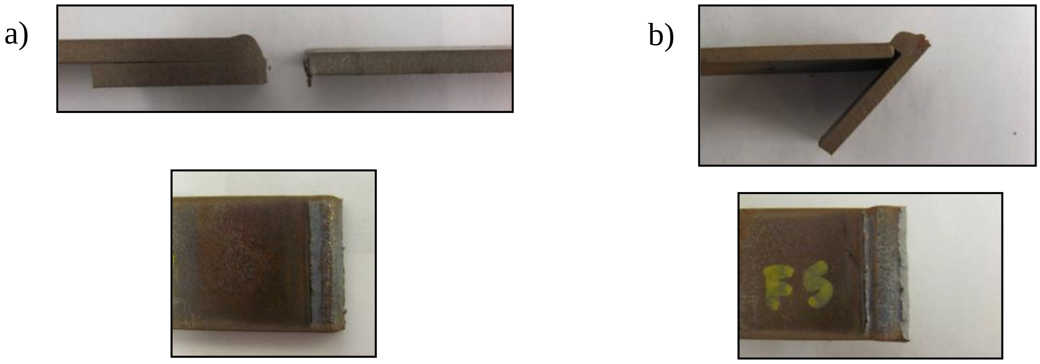

Fig. 12 Failure Location at Side and Top View a) Weld Toe b) Weld Toe-Root

In the case of the fatigue test an analysis with scanning electron microscopy SEM, evaluation of the fracture surface fatigue specimens, show no significant effect on the mode and propagation of the fracture due to the different fatigue loads applied, or the effect of different heat inputs used, showing ductile fracture rate in all samples tested as shown in Fig 13 and 14.

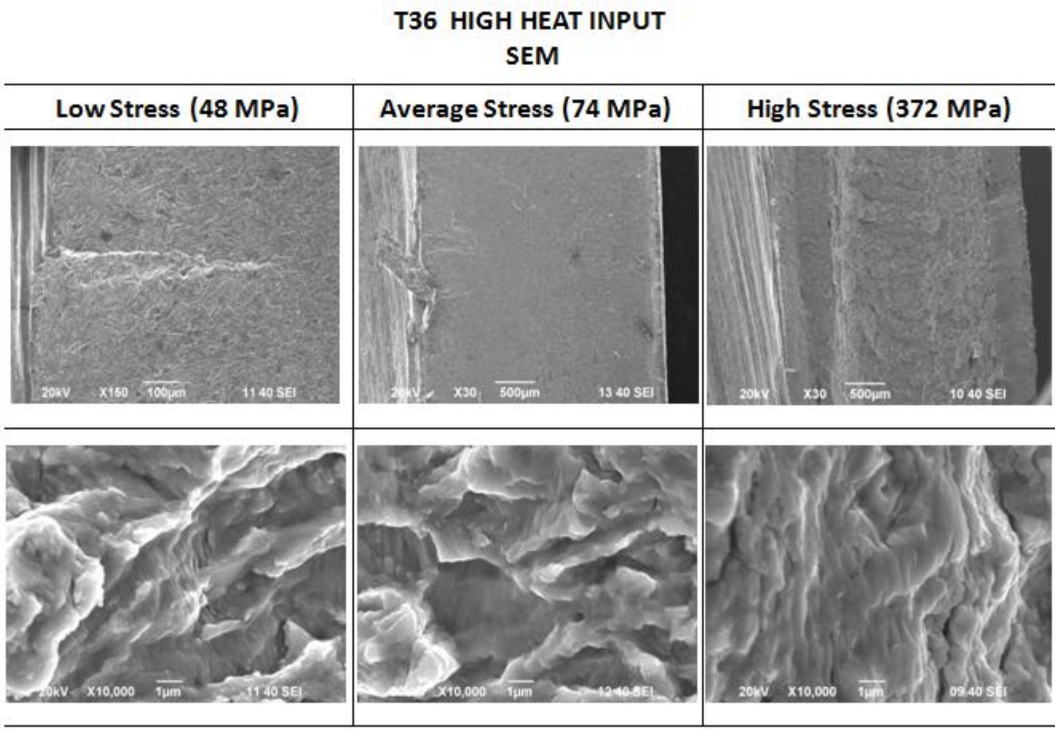

Fig. 13 SEM Fracture surface spécimen T36 différent stress

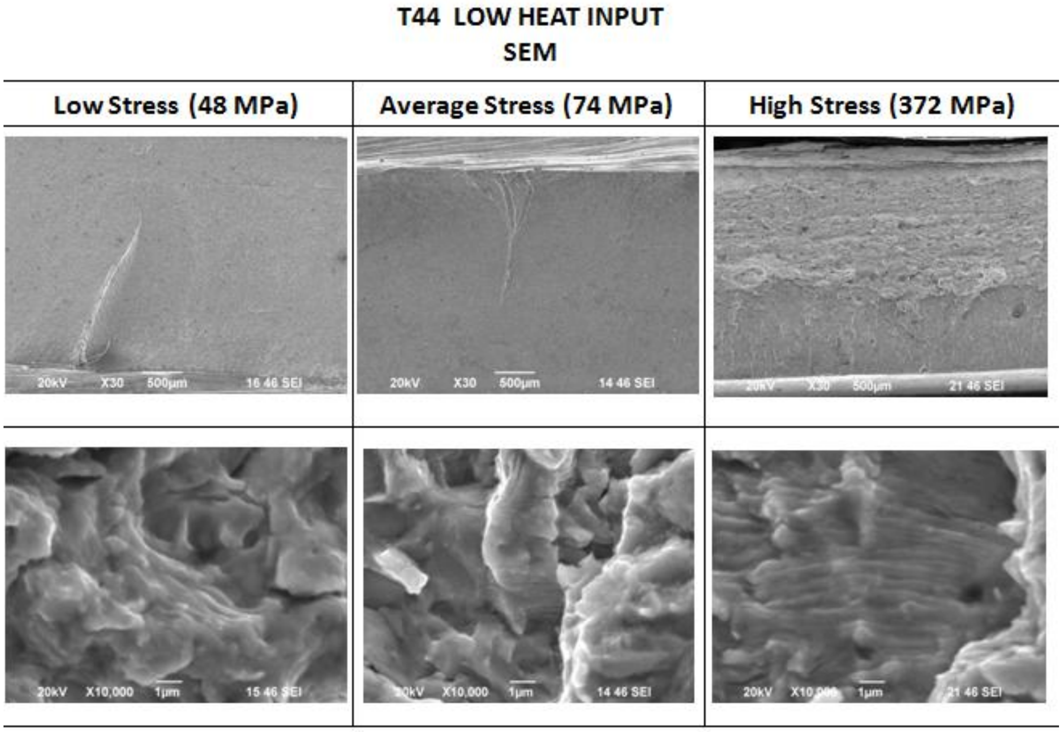

Fig. 14 SEM Fracture surface spécimen T44 différent stress

3.4 Metallograpy

Microstructural analysis was performed in the base metal AHSS steel TRIP 780 before being welded, having a multiphase microstructure mainly composed of ferrite, bainite and traces of retained austenite as shown in Fig. 15

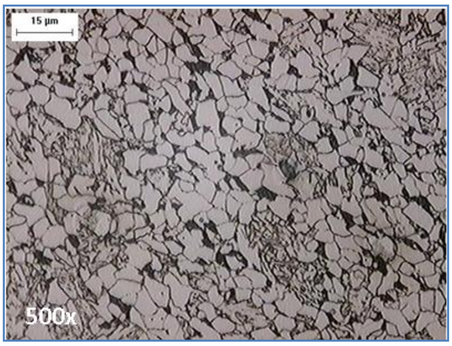

Fig. 15 Microstructure AHSS steel TRIP 780

In Fig. 16 and 17 show the metallography of the Base Metal (BM), Softening Zone (SZ), Heat Affected Zone (HAZ) and Weld (W) for the different heat input conditions evaluated. The microstructural characteristics of TRIP steel in their condition before being welded shown in Fig. 3a and 4a. Where there is a mixture of ferrite, bainite and some traces of retained austenite.

In Fig. 3b and 4b the SZ is coarse ferrite grains in addition to a greater percentage of particles that are formed granular bainite colonies that grow thicker and thickness is increased as a percentage of the heat input as shown in Fig. 3b, also traces of retained austenite, this zone being the one with the lowest values of hardness due to this thermal effect introduced by the heat input during the welding process and reduced cooling rate, which promotes microstructural phase precipitation as soft ferrites and thick bainites, being the highest heat input T36 specimen which has greater sensitivity to the effect of softening.

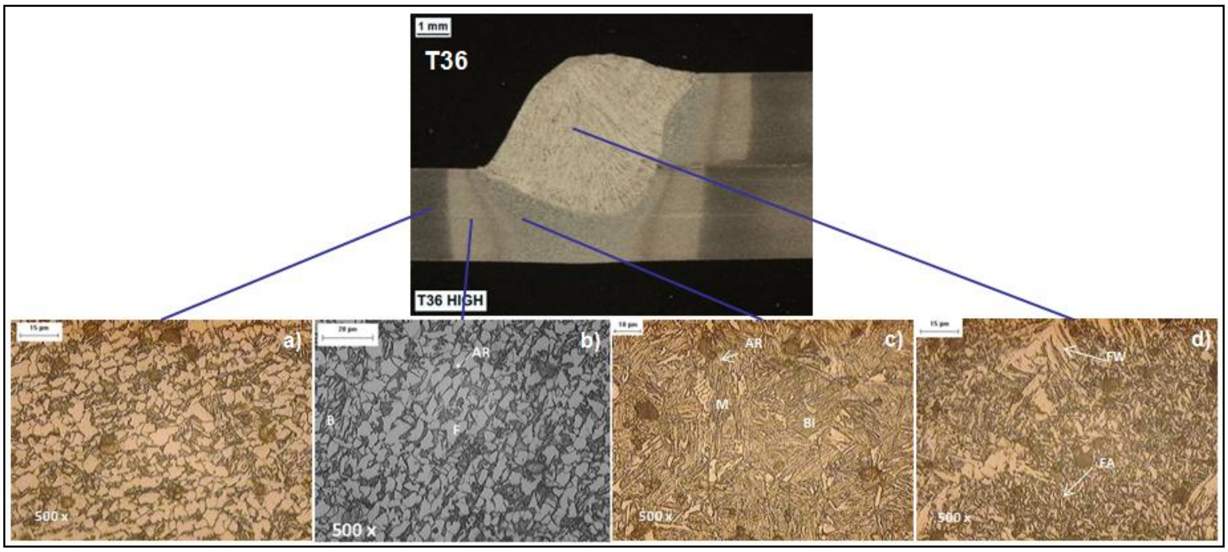

Fig. 16 Microstructures specimen T36 High HI a) BM b) SZ c) HAZ T44 d) Weld

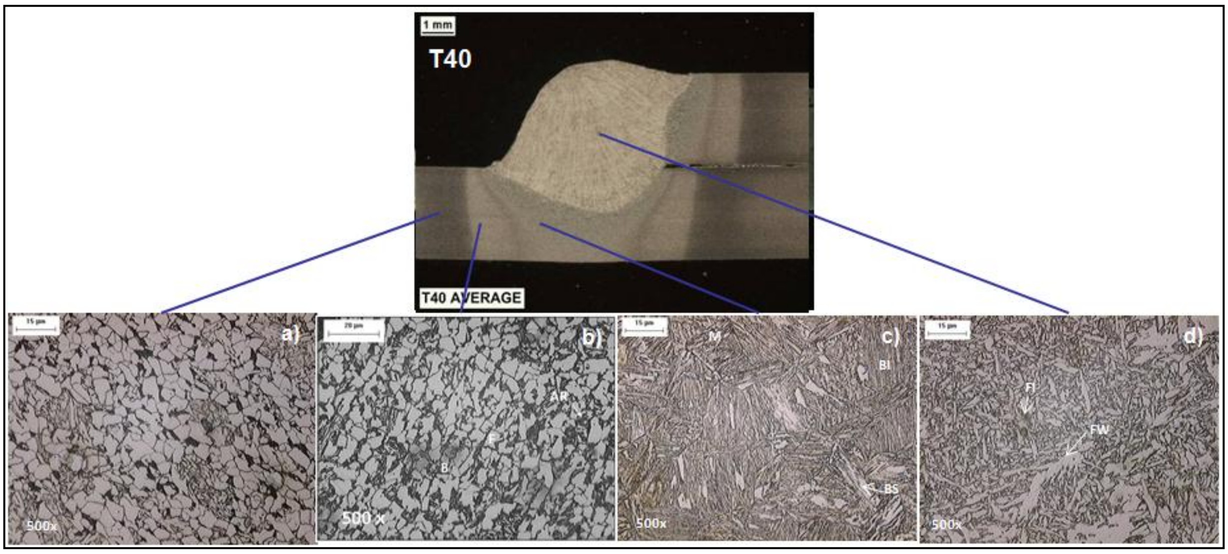

Fig. 17 Microstructures specimen T44 Low HI a) BM b) SZ c) HAZ T44 d) Weld

During the welding process due to the high cooling rates carbon steels and low alloy tend to be hardened and in the HAZ microstructure exhibits the same trend. The HAZ close to the weld is completely austenite and due to the different ranges of cooling martensitic structures (very high cooling rates), ferrites and bainites (high cooling), ferrite (low cooling rates) are formed during cooling. Figures 3c and 4c, are observed martensite and lower bainites, some traces of retained austenite, that as the heat input decreases, the cooling rate increases favoring the presence of finer bainites with greater hardness, as shown in T44 specimen, being in this area has the highest hardness of the weld joint. The weld zone has a columnar grained microstructure typical filler metal mainly consisting of acicular ferrite at grain boundary, and Widmanstatten ferrite see Fig. 3d and 4d.

3.5 X-Ray Diffraction (XRD)

The diffraction patterns of the samples are shown in Fig. 18 the austenite and ferrite peaks are clearly marked. Austenite peaks are rather low for the samples. Furthermore, the austenite peaks for the samples are similar, so that the amount of austenite will be similar. For the calculations of retained austenite, it is important to use an averaging method for any unique combination of peaks of austenite / ferrite that is prone to error due to the preferred orientation. Therefore, in the data shown below, four values were calculated using the peak austenite 111 austenite and ferrite peaks 110, 200, 211 and 220.

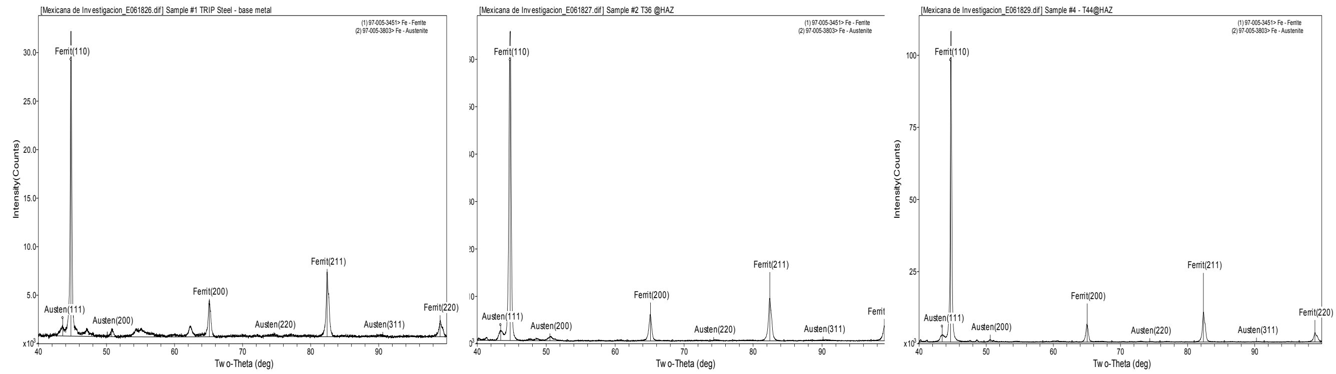

Fig. 18 XRD Pattern at HAZ a) Base Metal b) High HI T36 c) Low HI T44

The other austenite peaks are too weak to be reliable, so no attempt has been made to extend the analysis to include these. Using this method, we have produced the following results show in the Table 3.

Table 3 Results Retained Austenite

Retained Austenite				
Sample	f^{γ}			
	Min. Value	Max. Value	Average	Standard Deviation
Base Metal	6.44	7.56	7.0	± 0.8%
T44 Low Heat Input	8.46	10.34	9.4	± 1.0%
T36 High Heat Input	9.60	12.99	11.3	± 1.5%

These results are consistent with Figure 18, where the sample T36 has the greatest peak austenite 111, while the base metal and T44 sample were found to have lower peak austenite. The standard deviations for the percent of retained austenite are most likely due to a small number of preferred orientations in the TRIP steel. Since the regions are tested in the HAZ, which do not undergo melting during welding. Therefore, they have retained the preferred orientation which existed before welding.

As we increase the amount of heat input also increases the volume fraction of retained austenite, which means that as we decrease the travel speed and increases the voltage and amperage increase the amount of retained austenite in the HAZ for these steels, the weld will feature a higher percentage of retained austenite in the weld joint and may transform to martensite during subsequent mechanical work producing higher strain hardening with consequent energy absorption for parts that are subject to impact. This can be seen in the relationship shown in Fig. 19.

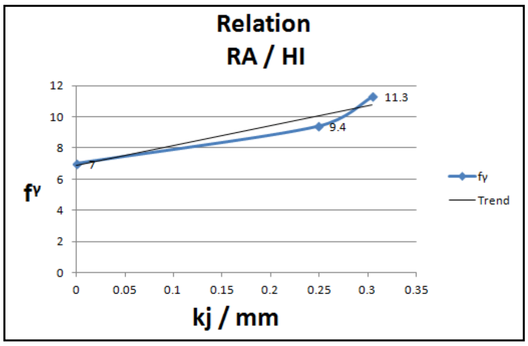

Fig. 19 Relation of the fraction of retained austenite and Heat Input

3. CONCLUSIONS

In order to study the effect of the heat input on the mechanical and metallurgical properties of the welds in TRIP steel welded with GMAW. Mechanical properties were evaluated with tension test, microhardness and fatigue testing and Metallurgical evaluation with optical metallograpy, Scanning electron microscopy fractograpy and X-ray Diffraction (XRD) to different Heat Input conditions concluding the following:

3.1 Mechanical properties

In tension test at shear stress as we increase the heat input, the resistance of the weld joint decreases in maximum load and shear strength, presenting a ductile failure mode at the root of the weld.

Microhardness testing shows the presence of a softening zone (SZ) that occurs in the transition in the base metal from the beginning of the heat affected zone (HAZ), in the three conditions tested presenting greater hardness loss as heat input increases. 232 HV sample T36, 235 HV sample T40 and 260 HV sample T44. The Heat Affected

Zone shows an increase in hardness as we decrease the heat input. 381 HV sample T36, 415 HV sample T40 and 446 HV sample T44.

In the fatigue test S-N curves for fatigue life were similar for all heat inputs, no significant differences at high loads and high nominal stresses, however at low loads and low nominal stresses evidenced greater variation between cycles obtained at low T44 and high T36 heat inputs, having a greater fatigue life welding specimens with mayor thermal effect by high heat input T36.

3.2 Metallurgical evaluation

Metallographic evaluation shows the presence of structures ferritic, bainitic and traces of retained austenite in both Metal Base (MB) and the Softening Zone (ZS) showing increase in both quantity and thickness of the ferrite and bainite colonies as we increase the heat input. The heat affected zone presents bainitic and martensitic structures with traces of retained austenite presenting finer structures, decrease the heat input and increases cooling rate causing an increase in hardness.

The sample with the highest heat input T36 (0304 KJ / mm) has the highest amount of retained austenite with a 11.3% increase on average 62% more than the originally obtained in the base metal 7% The sample with the lowest heat input T44 (0,248 KJ / mm) has also increased the amount of retained austenite with a 9.4% increase in average 34% more than the originally obtained in the base metal 7%.

This leads us to conclude that these conditions study the content in volume fraction of retained austenite increases in the HAZ of welds with increasing heat input into the base metal due to thermal effects caused by the heat supplied by the GMAW welding process, which provides a greater amount of retained austenite in the weld joint to be transformed to martensite during the following forming process of the parts or during the absorption of energy during a sudden impact.

REFERENCES

Kapustka N, Conrardy C, Babu S., y Albright C., (2008), Effect of GMAW Process and Material Conditions on DP 780 and TRIP 780 Welds, American Welding Society and the Welding Research Council, pp 135 – 148. USA

Mei Zhang, Lin Li, Ren-Yu Fu, Ji-Cheng Zhang, Zi Wan, (2008), Weldability of low carbon transformation induced plasticity steel, Journal of Iron and Steel Research, International, Vol. 15(5), pp. 61-65.

LI Zhuang, LV Hui-sheng, F Shi-rong Continuous Cooling Transformation Behaviour of C-Si-Mn TRIP Steel. Proceedings of Sine Swedish Structural Materials Symposium 2007.

Zhao L., Wibowo M.K., Hermans M.J.M., van Bohemen S.M.C. Sietsma J., (2009), Retention of austenite in the welded microstructure of a 0.16C-1.6Mn-1.5Si (Wt.%) TRIP steel, Journal of Materials Processing Technology 209, pp 5286-5292.

Han Tae-Kyo, Park Sin Sang, Kang Chung-Yun, Woo In-Su, Lee Jong-Bong, (2005), CO2 laser welding Characteristics of 800 MPa class TRIP Steel, ISIJ International, Vol. 45 (2005), pp. 60-65.

Zhao, L., Van Dijk N.H., Bruck E., Sietsma J., Van Der Zwaag S.,(2001). Magnetic and X ray diffraction measurements for the determination of retained austenite in TRIP steels.material Science and Engineering A313, pp 145-152.
Lopez V.H., Perez G., Reyes A., Lopez H.F., (2010), Effects of heat input in the mechanical integrity of the weld joints welded by GMAW and LBW process in transformation induced plasticity steel (TRIP) used in automotive industry, Soldagem and Inspecao, Vol. 15, No. 3, pp. 234 – 241, Sao Paulo, Brasil.
Zhang Mei., LI lin and FU Ren yu. (2008), "Weldability Low Carbon Transformation Induced Plasticity Steel", Journal Iron and Steel research *International.*
Zhili Feng., Yang Sang and Chonghua Jiang. (2009), "Fatigue performance of advanced high strenght steel AHSS GMAW Joints ", *Society of Automotive Engineers SAE.,* 2009-01-0256.
I.D.Choi et al. „Deformation behaviour of low carbon TRIP sheet steels at high strain rates'. ISIJ Int 2002; 42(12):1483–9; 2002.
J. E., Gould, L. R. Lehman, S. Holmes. „A design of experiments evaluation of factors affecting the resistance spot weldability of high-strength steels'. Proc. Sheet Metal Welding Conference VII, AWS Detroit Section, 1996.
J. E., Gould, D. Workman, „Fracture morphologies of resistance spot welds exhibiting hold time sensitivity behavior'. Proc. Sheet Metal Welding Conference VIII, AWS Detroit . 1998.
Bhadeshia, H. K. D. H; and Svensson, L-E 1993. Mathematical Modeling of Weld Phenomena, eds, H. Cerjack and K. E. Easterling, Institute of Metals, London, pp.109-180.
Li, M. V; Niebuhr, D. V; Meekisho, LL and Atteridge, D.G.1998. „A computational model for the prediction of steel hardenability'. Metallurgical and Materials Transactions 29B (6):661- 672.
J.E. Gould, S.P. Khurana, T. Li; „Predictions of microstructures when welding automotive advanced high-strength steels'; Welding Journal, AWS, May 2006, 111.
M Kuo,Y Sang, Ch Jiang, J Chiang, Z Feng. Fatigue Performance of Advanced High-Strength Steels (AHSS) GMAW Joints. SAE Paper 2009-01-0256.
LI Zhuang, LV Hui-sheng, F Shi-rong Continuous Cooling Transformation Behaviour of CSi-Mn TRIP Steel. Proceedings of Sine Swedish Structural Materials Symposium 2007.